



# Large Scale Tests on Bridge Slabs Cantilevers Subjected to Traffic Loads

**Vaz Rodrigues, R., Muttoni, A. Prof. Dr., Burdet, O. Dr.**

*Structural Concrete Laboratory, Ecole Polytechnique Fédérale de Lausanne, CH-1015 Lausanne, Switzerland*

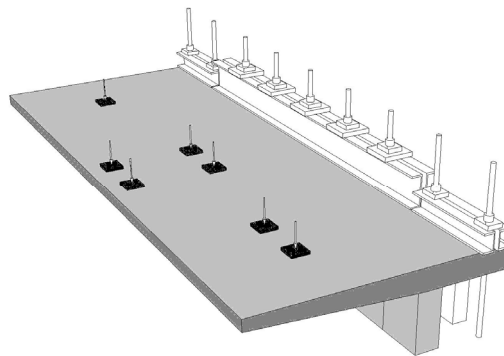
## INTRODUCTION

The load carrying capacity of deck slabs under high traffic loads is an important issue in bridge safety. The design of bridge slab cantilevers is commonly made using either elastic calculations or yield-line theory. However, under high traffic loads, as the large rotations required for the full development of the yield-line mechanism affect the shear strength of the slab, a premature and brittle shear failure can occur. An experimental and theoretical investigation of the shear strength of reinforced concrete slabs without shear reinforcement is under way at the Ecole Polytechnique Fédérale de Lausanne. The first part of the experimental program consisted of shear tests on twelve slab strips without shear reinforcement, with a constant reinforcement ratio of 0.79%, an overall depth of 450 mm and total length of 8 400 mm. All the slab strips except one failed in shear, at various levels of plastic strains in the longitudinal reinforcement. The test results show that the shear strength decreases with increasing plastic hinge rotation. A description of the obtained results is exposed in [1] and [2].

The second part of the experimental program part consists of tests on large scale reinforced concrete bridge cantilevers without shear reinforcement, with an overall depth of 0.38 m at the fixed end, a span of 2.78 m and a length of 10 m. The cantilevers are tested under different configurations of concentrated loads simulating traffic loads. The observed mode of failure is shear. This paper presents the first experimental results for the large scale bridge cantilevers. The large scale tested cantilever is shown under the loading patterns in fig. 1 b).



a) Bridge girder with cantilever



b) Large scale model under loading patterns (2.78 m cantilever)

**Fig. 1.** Bridge girder and large scale model.

**Keywords:** Shear strength without transverse reinforcement, yield-line, bridge deck cantilevers, traffic loads, rotation capacity

## TESTS ON LARGE SCALE BRIDGE CANTILEVERS

The tested cantilever is a 3/4 model of a full scale bridge cantilever. The full scale cantilever was designed using the traffic loads prescribed by Eurocode 1 ([5]), and the scale factor was applied keeping the same reinforcement ratios than in the full scale structure. Despite the scale factor, the dimensions of the tested cantilever (2.78 m span x 10.0 length) are representative of cantilevers of large concrete box girders.

### Test setup and material properties

The cantilever has a span of 2.78 meters (distance from the fixed end to the tip of the cantilever) and a total length of 10.0 meters. The test concept and the load arrangement are shown in fig. 2. The slab thickness varies from 0.38 m at the fixed end to 0.19 m at the cantilever tip. The main reinforcement of the top layer at the fixed end consists of 16 mm diameter bars at 75 mm spacing, which corresponds to a reinforcement ratio of 0.79%. Figure 3 shows the reinforcement layout and the cantilever dimensions, along with the position of the concentrated loads simulating vehicle wheels. The bottom reinforcement consists of 12 mm diameter bars at 150 mm spacing in both directions. The concrete cover is 30 mm.

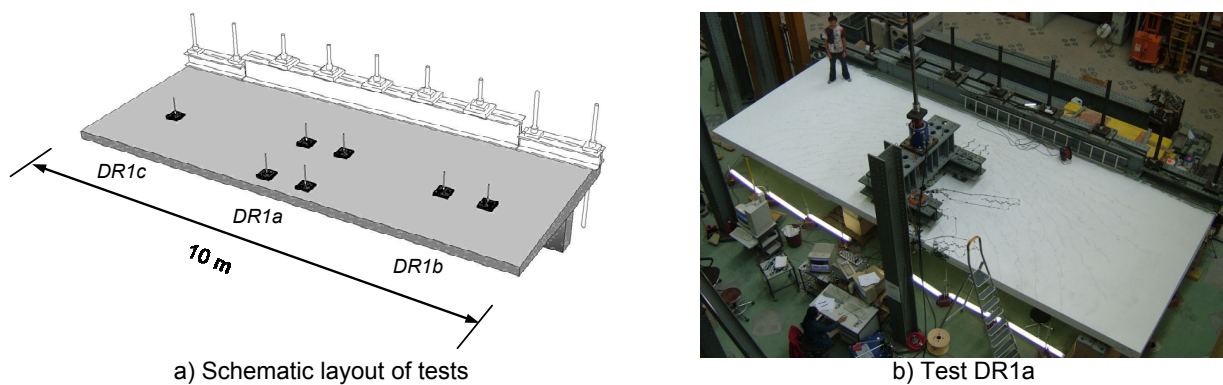


**Fig. 2.** Test concept and load arrangement.

The applied loads for the first test (DR1a) are the twin axle loads prescribed by Eurocode 1 with all dimensions reduced by 3/4. The subsequent tests (DR1b and DR1c) were performed using only two, resp. one concentrated load to better focus on shear and punching shear failure modes. The concentrated loads were applied on the top of the slab using steel plates with dimensions 300 x 300 x 30 mm.

The fixed end support was clamped by means of a vertical prestressing (7 MN total force). The concentrated loads were applied through holes ( $\varnothing$  130 mm) in the slab, which allowed to pull directly from the strong floor (fig. 2 and 3).

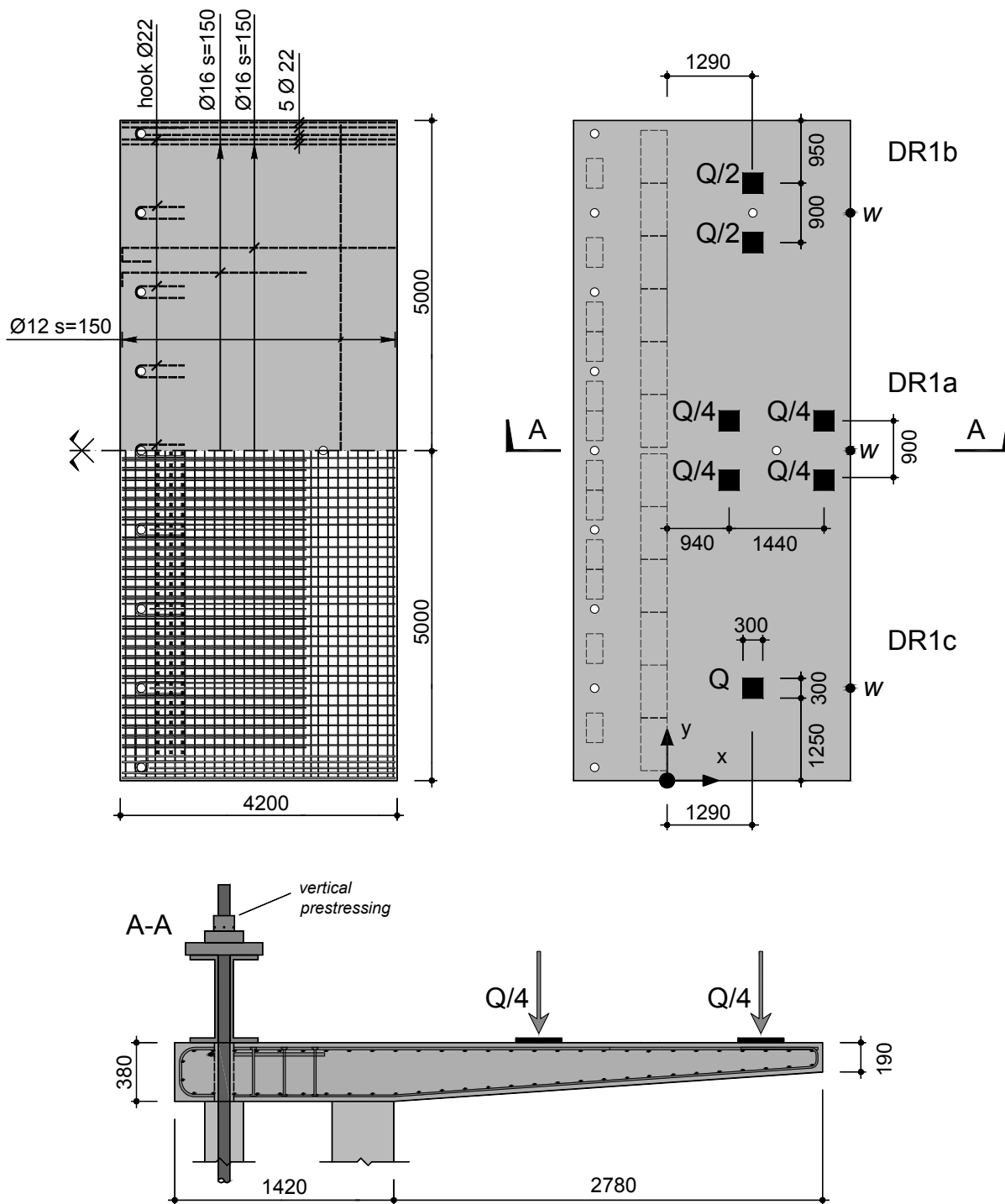


**Fig. 3.** Slab dimensions, reinforcement layout and applied loads for the tests. Dimensions in mm.

Table 1. gives the main material properties at the time of testing.

**Tab. 1.** Concrete properties for tests DR1a, DR1b and DR1c  
Maximum aggregate size 16 mm

| Test | $f_c$ [MPa] | $E_c$ [GPa] |
|------|-------------|-------------|
| DR1a | 39.0        | 36.0        |
| DR1b | 39.9        | 36.1        |
| DR1c | 40.8        | 36.2        |

The reinforcement steel used is hot-rolled, with a yield strength of 515 MPa for bars with 16 mm and 22 mm diameter, and of 535 MPa for bars with 12 mm diameter.

### Experimental results

**Tab. 2.** Experimental results

| Test | Number of wheel loads | Failure Load $Q_R$ [kN] | Theoretical Flexural Failure Load $Q_{Flex}$ [kN] | $Q_R/Q_{Flex}$ | Failure location | Mode of failure |
|------|-----------------------|-------------------------|---|----------------|------------------|-----------------|
| DR1a | 4                     | 1380                    | 1600  | 0.86           | Cantilever edge  | Shear           |
| DR1b | 2                     | 1025                    | 1320  | 0.78           | Fixed end        | Shear           |
| DR1c | 1                     | 937                     | 1190  | 0.79           | Fixed end        | Shear           |

The results of the 3 tests are summarized in Table 2. The failure mode for the cantilever under four concentrated loads (DR1a) was a brittle shear failure at the two loads near the edge (fig. 8). For the other 2 tests (DR1b and DR1c) the cantilever also failed in shear, however at the region located between the applied loads and the fixed end of the cantilever. Calculations were made of the theoretical yield-line failure load, based on the upper bound theorem of limit analysis. The corresponding configurations of the yield-lines are shown in fig. 4. The yield-line analysis includes the effect of variable depth, orthotropic reinforcement and discontinuity of the main reinforcement in the top layer. A comparison with results of calculation of the ultimate load with a non-linear Finite Element program showed that the results obtained by the yield-line method are close to the theoretical flexural failure load. This load was never reached in any of the three tests.

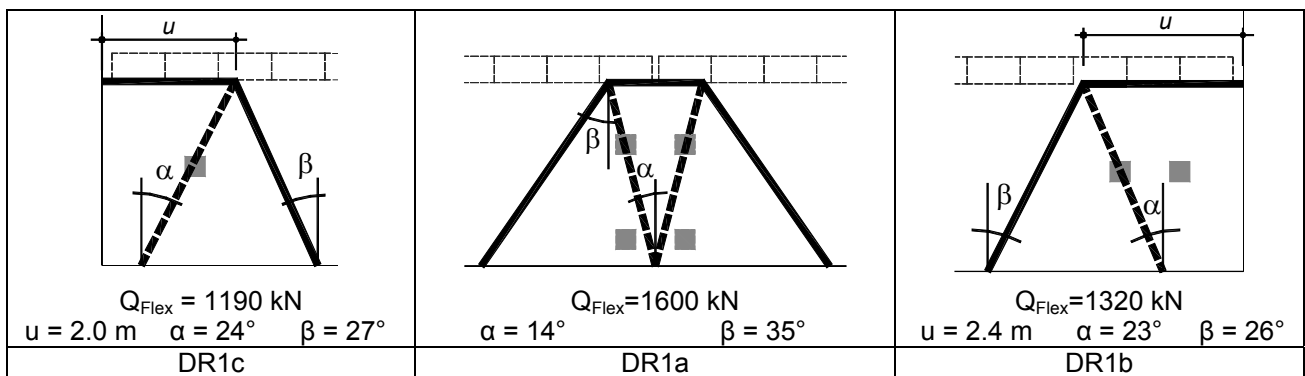


**Fig. 4.** Yield-line mechanisms and yield-line failure load ( $Q_{Flex}$ ).

The failure load in test DR1a with four concentrated loads is closest to the theoretical yield-line values ( $Q_R/Q_{Flex} = 0.86$ , Table 2). In this case, some plastic strains were present in both the top reinforcement at the fixed end (bars along x) and the bottom reinforcement below the edge loads (bars along y). At these locations, the surface crack openings observed close to failure were approximately 1.2 mm and 1.0 mm. The failure mode was clearly a brittle shear failure and not a flexural one. In the other two tests, little or no yielding occurred before failure in shear.

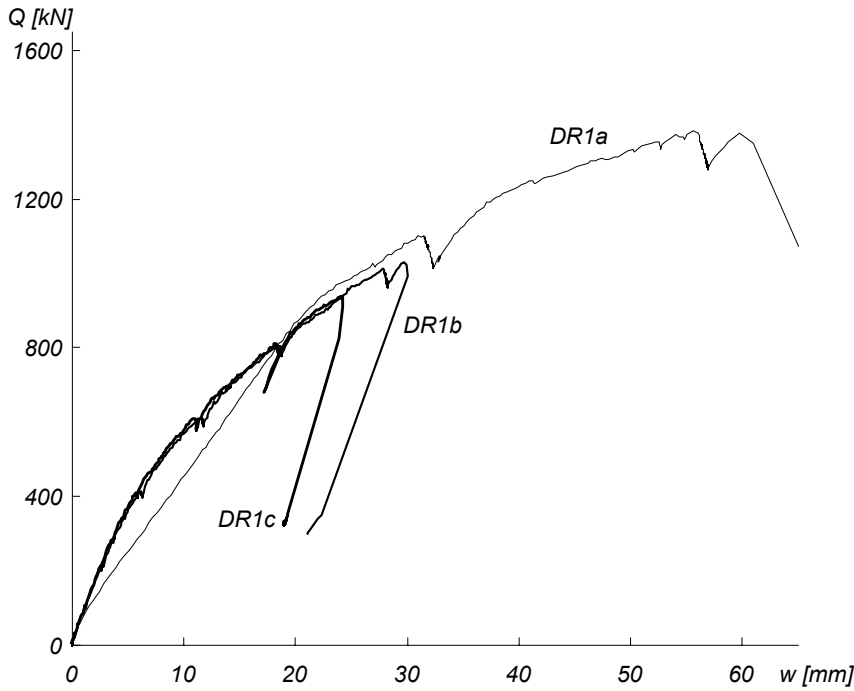


Fig. 5. Total load – deflection curves for the 3 tests.

The load-deflection curves for the three tests are shown in fig. 5. The deflection  $w$  was measured at the tip of the cantilever as indicated in fig. 3. The behavior of all tests is brittle, with a sudden failure in shear. There is no observable ductility, which is confirmed by the fact that only limited yielding of the flexural reinforcement occurred. The deflections of test DR1a are larger due to the load configuration with two loads close to the edge of the cantilever.

The behavior of the cantilever under cyclic loading for a low number of cycles was investigated before conducting the DR1a failure test. The results of 100 cycles with amplitude of 410 kN are plotted in fig. 6. The deflection at the tip of the cantilever increases with increasing cycles. This tendency was clearly observed in the first 50 cycles, but the deflection appears to have stabilized at the end of the 100 cycles (fig. 6b). The maximum crack width reached about 0.15 mm at 410 kN and 0.08 mm at 0 kN, at the top surface of the fixed end of the cantilever. After the cyclic loading, the cantilever was taken to failure. The deflection  $w$  for test DR1a in fig. 5 does not include the residual deflection due to the cyclic loading.

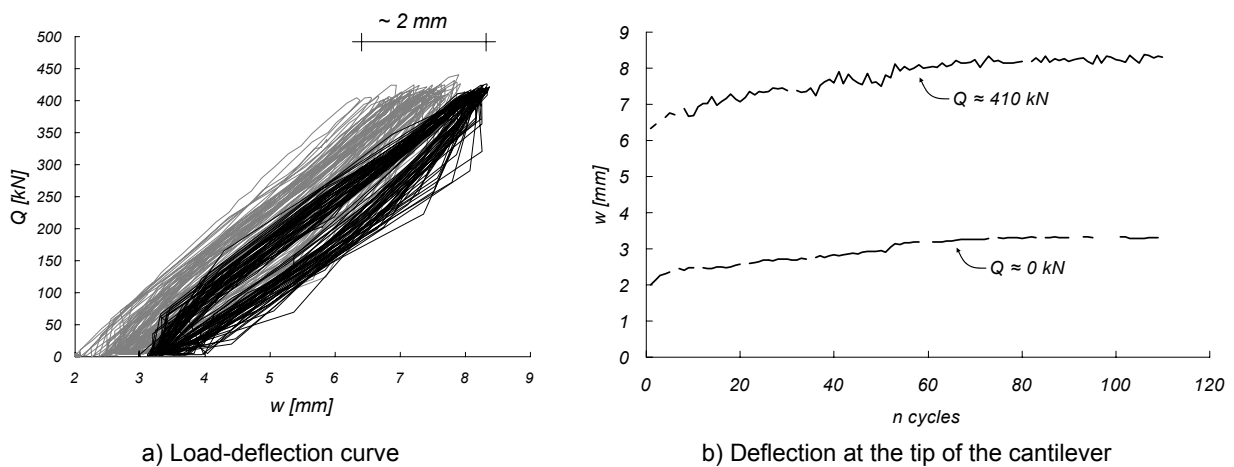
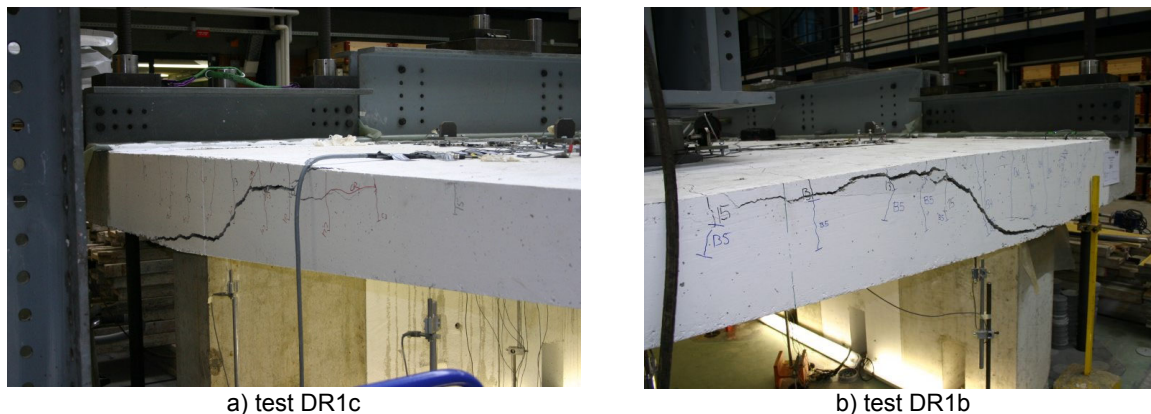


Fig. 6. Effect of 100 cycles on the deflection at the tip of the cantilever, DR1a.



**Fig. 7.** Shear failure at the fixed end of the cantilever

Figure 7 shows the shear failures obtained for the case of tests DR1b and DR1c. The shear crack was clearly visible after failure on the side face of the cantilever and the crack continues inside of the slab. After failure the slab was cut and the geometry of the critical crack was mapped. The crack patterns on the top and bottom surfaces for tests DR1b and DR1c are shown in figs. 10 and 11.

The observed crack pattern prior to failure at the cantilever top face is shown in fig. 8 for test DR1a. The first cracks were visible on the top surface at the fixed end for  $Q = 180$  kN. At this location the average crack spacing was of about 0.15 m. Cracks appeared also on the bottom surface, mainly aligned with the x axis and spaced by 0.15 m. Figure 9 shows that the shear failure took place near the cantilever edge. A large shear crack was also observed in the region between the fixed end and the applied loads. Since no failure occurred in this region, this suggests that a process of development of the shear crack was under way in this region and that redistributions of the shear flow may have occurred. In order to better follow the development of the shear crack, measurements of the shear crack openings inside the slab will be performed in the next series of tests.

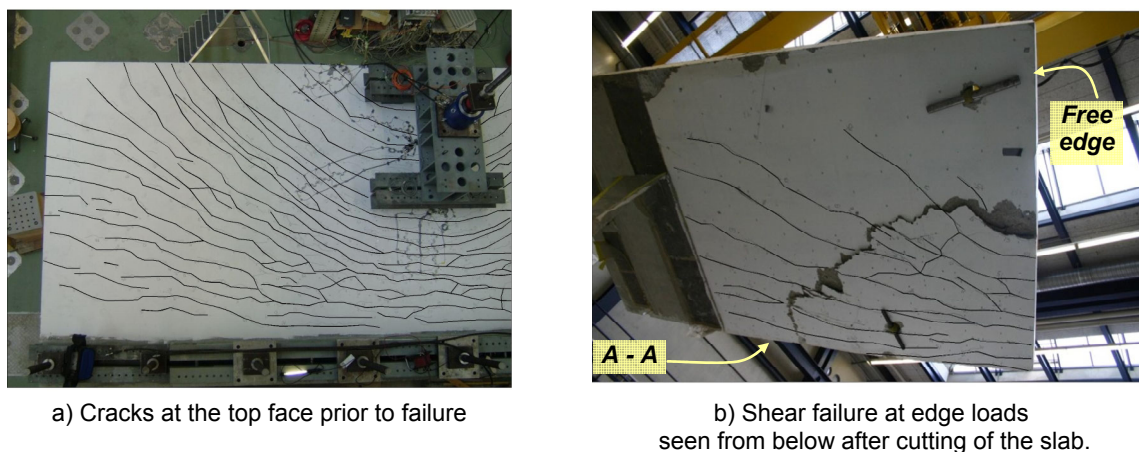


**Fig. 8.** Cracks and shear failure, DR1a.

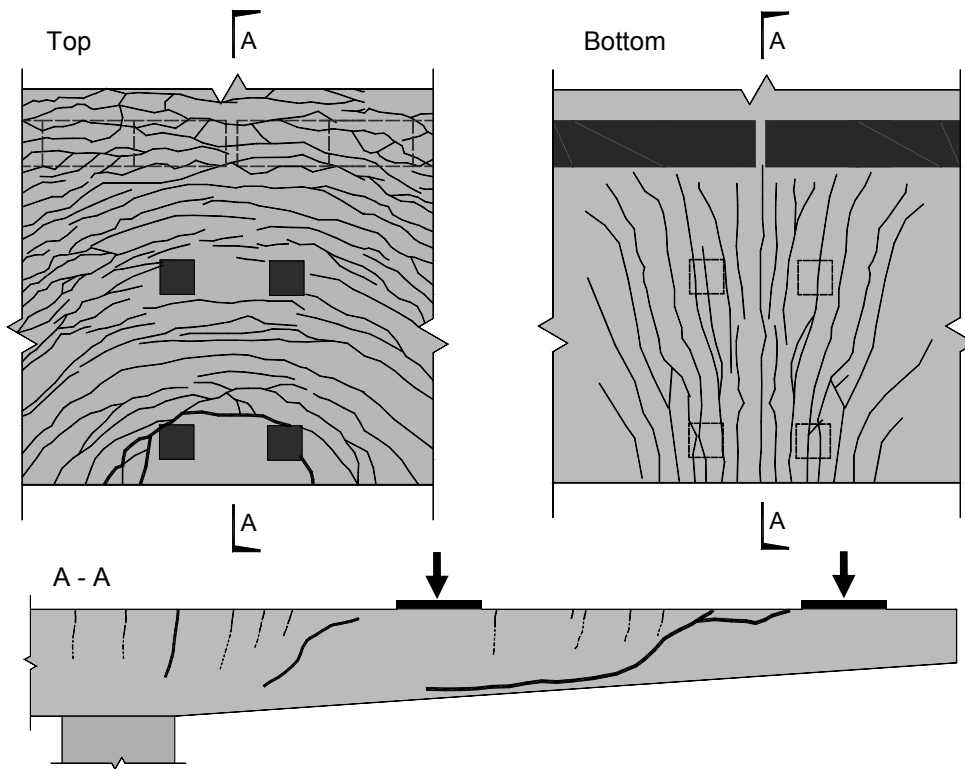


Fig. 9. Crack pattern on the top and bottom surfaces for test DR1a

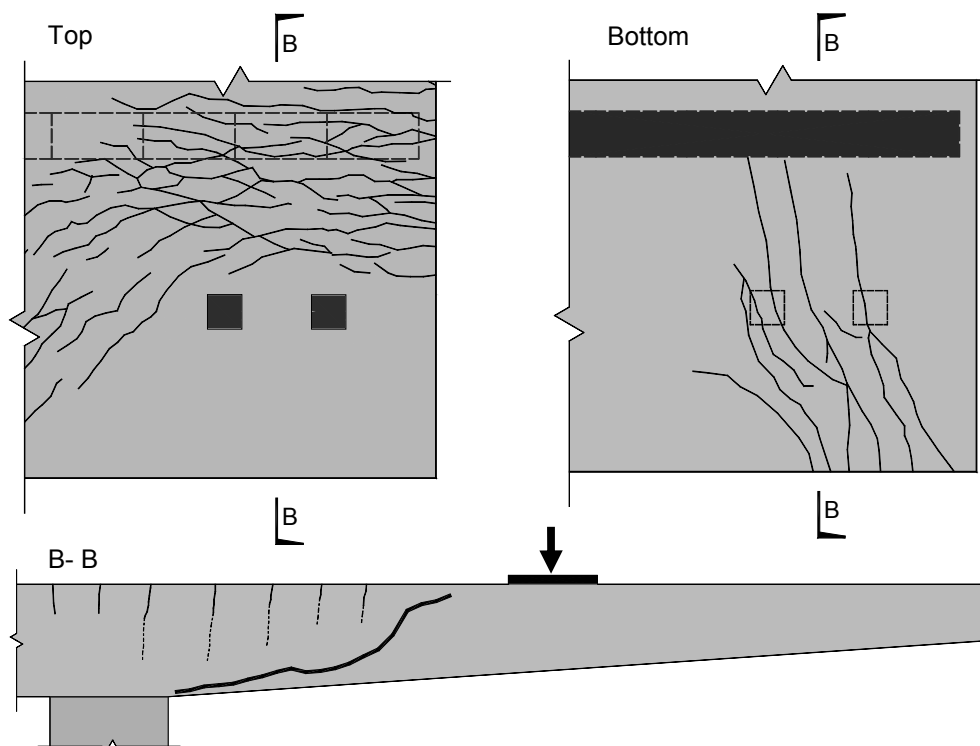
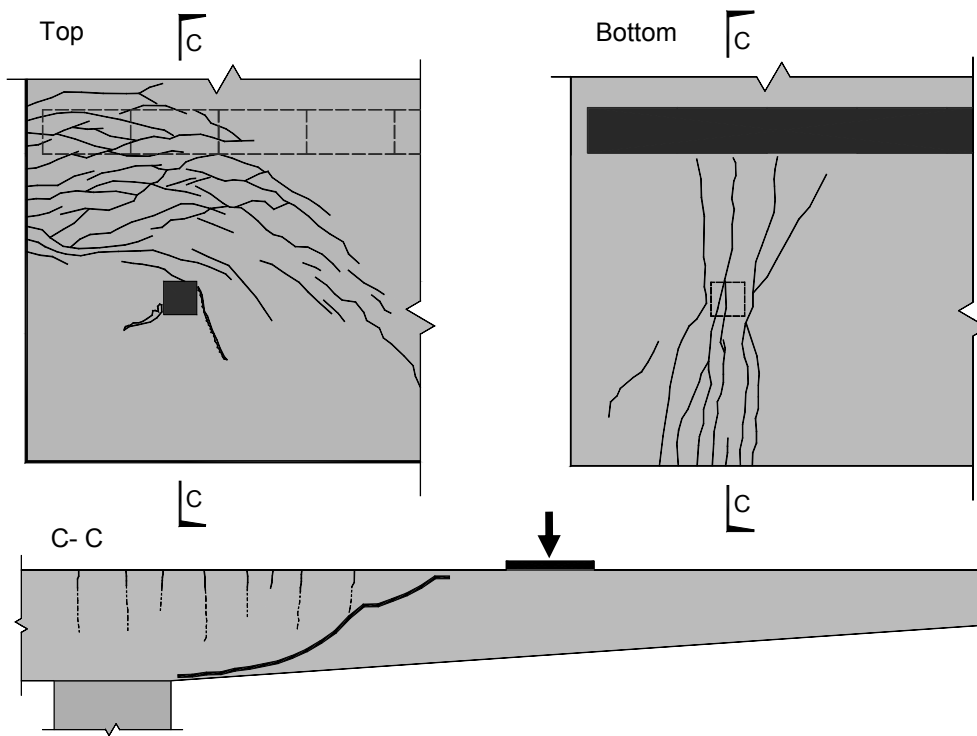


Fig. 10. Crack pattern on the top and bottom surfaces for test DR1b.



**Fig. 11.** Crack pattern on the top and bottom surfaces for test DR1c.

Test DR1a caused flexural cracks on almost the entire top surface of the cantilever. However, the crack openings remained small (about 0.05 mm) in the regions where the two following tests were performed. The cracks shown in figs. 10 and 11 are the new cracks and those whose openings grew during the corresponding tests.

### SHEAR FLOW

The observed failure modes of tests DR1a to DR1c are intermediate cases between shear in beams without shear reinforcement and punching shear of flat slabs. It is therefore useful to investigate both of these modes of failure and to see if a relationship can be found between them.

The shear flow is a representation of the direction  $\varphi_0$  and amplitude  $v_0$  of the principal shear force in slabs, given by eq. (1) and (2) (Marti [6]).

$$\varphi_0 = \arctan \left( \frac{v_y}{v_x} \right) \tag{1}$$

$$v_0 = \sqrt{v_x^2 + v_y^2} \tag{2}$$

This representation is not commonly used to display the results for FE calculations, but it is a useful tool to investigate the problem of shear in cantilevers. Figures 12 and 13 show the linear elastic shear flow direction and lines of equal principal shear forces for all three tested configurations. Also shown in the figures are the areas of principal and secondary shear cracking.



Two regimes can be observed: in the case of test DR1a, the failure occurred in an area of strong gradient of the shear flow, similar to a punching failure, while a secondary cracking area developed in another area of more constant shear flow. In the other two cases, the failure occurred in areas of more or less constant shear flow, similar to a shear failure.

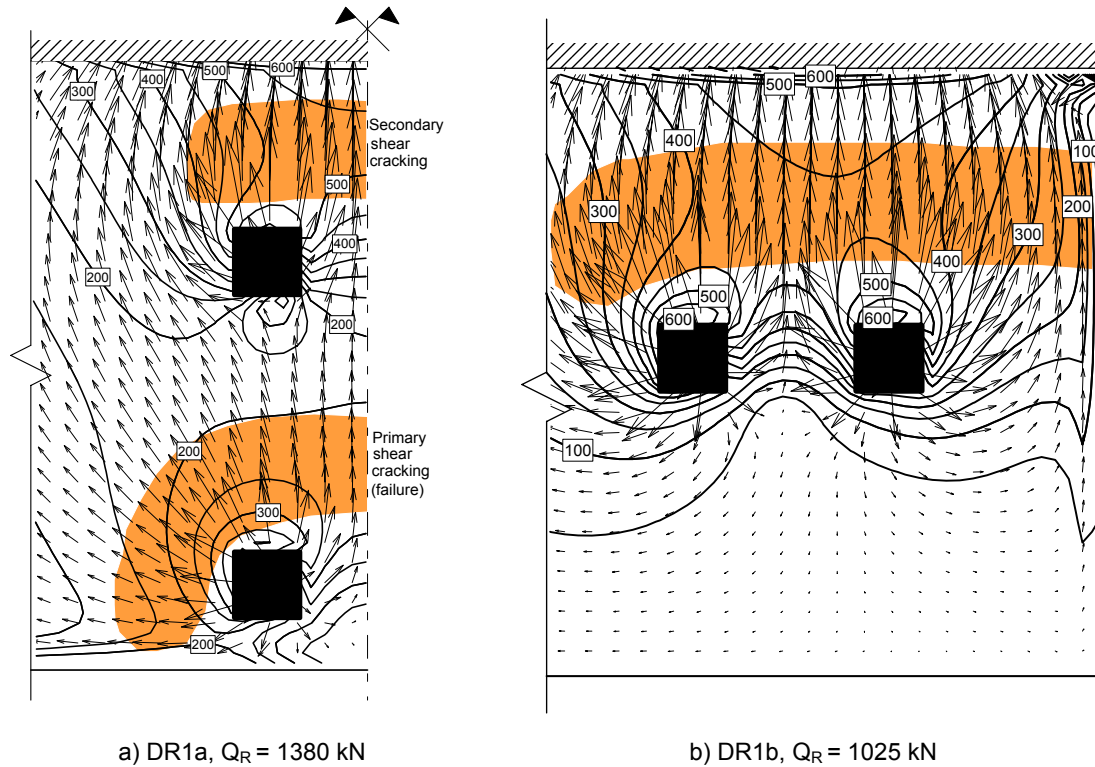


Fig. 12. Shear flow directions and contour curves of  $v_0$  [kN/m].

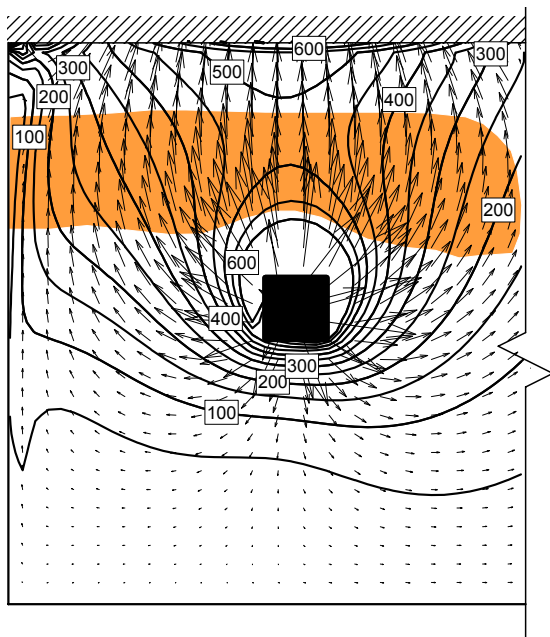


Fig. 13. Shear flow and contour curves of  $v_0$  [kN/m], DR1c,  $Q_R = 937$  kN.

## CONCLUSIONS

This paper describes the results obtained on three large scale tests of a reinforced concrete bridge cantilever under concentrated loads. The following conclusions can be made:

- Bridge cantilevers without shear reinforcement tend to fail in shear under concentrated loads.
- The ultimate load calculated by the yield-line method was not reached for any of the three tests. The ratio between the failure load and the theoretical yield-line failure load was higher with four concentrated loads than with two or one concentrated loads.
- Important flexural and shear cracks occurred near the fixed end of the cantilever, but the shear failure did eventually occur at location closer to the edge loads. This suggests possible redistributions of the internal shear flow, with the progressive formation of shear cracks until equilibrium is no longer possible.

The available results should contribute to a better understanding of shear and punching shear as similar phenomena.

## ACKNOWLEDGEMENTS

The authors would like to express their gratitude to the Swiss Federal Roads Authority (FEDRO) and to the Portuguese Foundation for Science and Technology (FCT) for their support.

## REFERENCES

1. Vaz Rodrigues R., Burdet O., Muttoni A. Experimental investigation of the shear capacity of plastic hinges, *Proc. of the fib symposium "Keep Concrete Attractive"*, vol. 2, pp. 651-656, Budapest, Hungary, May, 2005.
2. Vaz Rodrigues R., Muttoni A. Influence des déformations plastiques de l'armature de flexion sur la résistance à l'effort tranchant des poutres sans étriers. Rapport d'essai, EPFL - IS-BETON, Lausanne, 2004 (<http://is-beton.epfl.ch/recherche/DalleRoulement/>).
3. Muttoni A. Schubfestigkeit und Durchstanzen von Platten ohne Querkraftbewehrung *Beton und Stahlbetonbau* 98, Februar 2003, Heft 2, pp.74-84.
4. SIA Code 262 (2003), Concrete Structures. Swiss Society of Engineers and Architects, 2003.
5. Eurocode 1: Actions on structures – Part 2: Traffic loads on bridges, EN 1991-2: September 2003.
6. Marti P. Design of Concrete Slabs for Transverse Shear. *ACI Structural Journal*, V.87, No. 2, March-April 1990.